Wireless Networks
https://doi.org/10.1007/s11276-023-03613-0

ORIGINAL PAPER

Polarization adaptation to improve cell border area bitrates and system capacity in small cells

Jukka Lempiäinen[1] · Muhammad Usman Sheikh[2] · Ari Asp[1] · Riku Jäntti[2]

Abstract
The target of this paper is to show the impact of polarization adaptation on the received signal quality in an outdoor small-cell deployment scenario. The signal-to-interference ratio (SIR) is the key factor in defining the achievable data rate, and the capacity of the cell. At the cell border area, the SIR value is typically low and causes a significant decrease in the system capacity and achievable data rates. These bad SIR areas at the cell border can be improved by using orthogonal polarizations in the neighboring cells rather than using all polarizations over the whole cell coverage area. For the research work of this paper, a series of measurements were carried out to measure a received signal power and a cross polarization discrimination (XPD) ratio while the signal is transmitted and received with a different set of polarizations. In the measurements, we have considered horizontal, vertical, +/− 45° slanted polarizations, and two different environments, urban street and open space, and three frequency bands, 970−1030 MHz, 2000−2030 MHz and 3364−3400 MHz. The measurement results revealed that at a different distance from the transmitter, for horizontal/vertical polarization, the average XPD is around 24.7 dB and 31.7 dB in the urban street and open area environments, respectively. For +/− 45° slanted polarization, the average XPD is around 11.5 dB and 12.1 dB in the urban street and open area environments, respectively. This paper goes on to propose polarization adaptation in each cell, where the primary polarization is valid for the whole service area of the cell, and secondary polarization is only used in close proximity of the base station antenna. Considering the results, it is emphasized that system capacity can be significantly improved by having only one channel with good SIR values compared to multiple channels with bad SIR values. However, MIMO channels with orthogonal polarizations or with spatial multiplexing can be utilized in the closed vicinity of the base station, i.e., in an area with good SIR values. It is shown that the overall cell capacity can be increased by almost 35% by utilizing polarization adaptation compared to MIMO 2 × 2.

Keywords Small cell · Cell densification · Polarization · System capacity · Cell border area

1 Introduction

Cellular systems as mobile networks are based on terrestrial radio propagation and the reuse of frequencies at neighbor base stations [1]. All available frequencies are typically used in all base stations as it yields the maximal potential system capacity [2]. Utilization of the same frequency in an adjacent cell causes co-channel interference, and that results in a decrease of the signal-to-interference ratio (SIR) as well as system performance. This deteriorated SIR happens especially in the middle of base stations, and those areas are called cell border areas. These cell border areas cannot be avoided, and the geographical size of these bad signal areas depends on the site grid, SIR

✉ Jukka Lempiäinen
jukka.lempiainen@tuni.fi

Muhammad Usman Sheikh
muhammad.sheikh@aalto.fi

Ari Asp
ari.asp@tuni.fi

Riku Jäntti
riku.jantti@aalto.fi

[1] Department of Communications Engineering, Tampere University, 33720 Tampere, Finland

[2] Department of Information and Communications Engineering, Aalto University, 02150 Espoo, Finland

Published online: 28 December 2023

requirement, radio propagation, and frequency. In heavily crowded and dense urban environments, lots of system capacity is required and thus lots of base stations are built in certain areas. Continuously increasing capacity requirements and higher frequencies of new technologies lead to dense base station site grids and small cells. In reference [3], it is shown that the system performance of densely implemented small cell infrastructure is squeezed as a function of site/cell distance. It is observed that the bad SIR area in between neighbor cells inversely increases as a function of site distance when the same frequency and polarization are used in neighbor cells. This is mostly due to the presence of a line-of-sight (LOS) component.

A typical approach in mobile network implementations follows the addition of technologies such as multiple-input-multiple-output (MIMO), where independent channels are established, e.g., based on orthogonality offered by different polarizations [4]. In bad-quality areas, MIMO is used for diversity to improve the SINR, whereas in good-quality areas, MIMO transmission with spatial multiplexing is utilized for enhancing the cell/user throughput [4]. Considering the radio propagation condition, with the adaptive MIMO switching (AMS) scheme, a better antenna transmission scheme is selected to maximize the user experience with better throughput and improved quality of service (QoS) [5]. The main target of MIMO with spatial multiplexing is to offer multiple independent bit streams and thus increase the overall system capacity. This approach of spatial multiplexing works fairly well in the proximity of the base station antenna where the SIR value is high and other MIMO-related radio conditions are good. However, lower bitrates are achieved for MIMO channels with bad propagation conditions and SIR [6–8]. Thus, MIMO with spatial multiplexing does not perform well in bad SIR areas, i.e., cell border areas, and therefore, it is recommended to switch between transmission modes considering the radio propagation condition [5]. Generally, in the case of MIMO systems, two different polarizations are used at the transmitter (TX) side. Moreover, the same polarizations are used in all cells of the system, thus causing strong interference and bad SIRs in the cell border areas.

In this paper, it is proposed to use orthogonal polarization in neighbor cells. In this case, signals received from neighbor cells have orthogonal polarization, and thus the strength of interference is comparatively lower than when using the same polarization in neighbor cells. The use of orthogonal polarization in the neighbor cell should be beneficial, especially at the cell border areas, and it is expected to offer remarkably higher data rates and capacity. However, both polarizations, i.e., MIMO with spatial multiplexing, can be used in close proximity of the BS, i.e., areas with good SIR values. Here, adopting single or dual polarization as a function of distance from the BS and SIR is called polarization adaptation. In this study, a measurement campaign was carried out to measure the received signal power while signals are transmitted and received with different polarizations. We have considered horizontal, vertical, +/− 45° slanted polarizations for this work. Later in the paper, capacity estimates are made for different polarization configurations considering the LOS environment and omnidirectional antennas at the TX and receiver (RX). This concept of adaptive polarization can be extended to other polarizations, e.g., orbital angular momentum (OAM) technique [9], as it also offers orthogonal channels with different polarizations and it is proposed for future mobile networks. Finally, this polarization adaptation approach is independent of mobile technologies, frequency bands, and environments.

2 Background theory

2.1 Radio propagation

In the case of small cells, base station antennas are placed below rooftop level and therefore, there is a high probability of having a line-of-sight (LOS) connection with mobile terminals as presented in Fig. 1. The attenuation of the radio signal in LOS connection follows a free space propagation. In such cases, a well-known free space path loss (FSPL) model [10] given in Eq. 1 can be used to estimate a minimum path loss, $PL_{FSPL,}$ between the TX and RX, where d is the spatial separation between the TX and RX in meters, and f is the center frequency in MHz.

$$\mathrm{PL_{FSPL}} = 10n\log_{10}(d) + 10n\log_{10}(f) - 27.55 \quad (1)$$

where n is a path loss exponent, and free space propagation has a path loss exponent of 2. Free space propagation does not involve any reflection or diffraction, and FSPL given in Eq. 1 is also independent of the polarization used at the TX or RX.

2.2 Polarization

Electric and magnetic fields have certain directions, and these directions specify the polarization of the electromagnetic field [11]. In the case of linear polarization, the electric and magnetic fields both have components in only one direction whereas circular and elliptical polarization have components in more than one direction. Moreover, the direction of the electric field defines the direction of polarization. In this paper, the main focus of our study is linear polarization. The traditional types of linear polarization used in a commercial mobile network are vertical, horizontal, and +/− 45° degree linear polarizations and

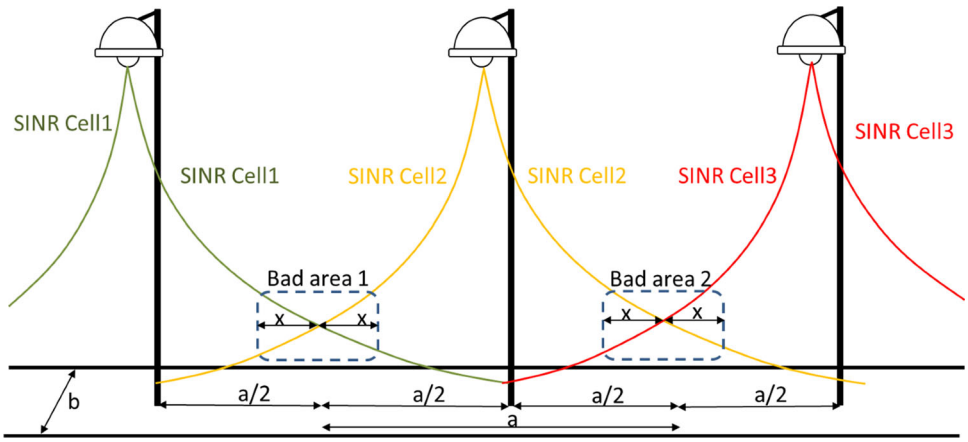

Fig. 1 Small cell deployment at a lamp post

elliptical and circular polarizations are commonly used in satellite communication.

In the case of fully orthogonal and uncorrelated polarization of the antenna used at the TX and RX, no signal is expected at the receiver, given that a polarization is not changed during the propagation path. In an open LOS environment, the polarization of the signal is not impacted. However, in a multipath-rich environment, i.e., an environment with multiple reflected, diffracted, and scattered paths, the polarization of each propagation path is changed with interactions with walls or other objects. Hence, the orthogonality of the polarization is compromised and therefore, a signal with lower strength is received at the receiver even though orthogonal polarization is used at the TX and RX. Figure 2 shows an example of a multipath-rich environment where several propagation paths exist between the TX and the RX. All signal components need to be considered to determine the behavior of the polarization.

This change from one polarization to another is related to cross polarization discrimination (XPD), i.e., the amount of polarization change. The cross polarization discrimination (XPD) is defined as the ratio of the received signal power with the desired polarization to the received signal power with the undesired polarization. The XPD, in dB value, can be computed by using Eq. 2, where Pr_i^D and Pr_i^U are the received power of the ith sub-carrier at the desired and undesired polarizations in dBm scale, respectively.

$$XPD = \sum_{i=1}^{k} \Pr_i^D - \sum_{i=1}^{k} \Pr_i^U \tag{2}$$

The reflection loss of perpendicular polarization, i.e., transverse electric (TE) fields, and parallel polarization, i.e., transverse magnetic (TM) fields, can be computed by using Eqs. 3 and 4, respectively [10], where, ε_r is the relative permittivity of the reflected material, and β is the

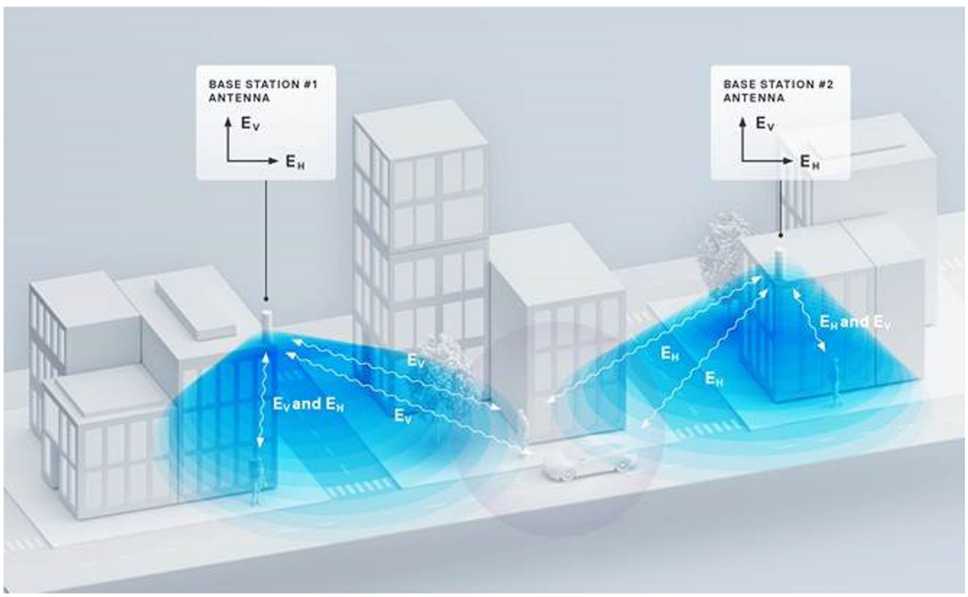

Fig. 2 Polarization adaptation

grazing angle. The TE and TM equations are valid for scenarios where the direction of the electric field is parallel and perpendicular to the plane of incidence, respectively. Thus, geometry has a huge impact on the polarization change together with the reflection coefficients. It should be noted that at high frequencies and in the LOS environment, the strength of diffracted paths has lower signal strength compared with LOS and reflected paths. In an LOS environment with cells utilizing the same frequency and polarization, the LOS path is the major contributor to interference between them, as presented in [3]. In the case of utilizing orthogonal polarization in immediate neighbor cells, the interference distance is three times (3×) longer for the base station utilizing omnidirectional directional antenna, as shown in Fig. 1.

$$R_{\mathrm{TE}} = \frac{\sin\beta - \sqrt{\varepsilon_r - \cos^2\beta}}{\sin\beta - \sqrt{\varepsilon_r + \cos^2\beta}} \tag{3}$$

$$R_{\mathrm{TM}} = \frac{\varepsilon_r \sin\beta - \sqrt{\varepsilon_r - \cos^2\beta}}{\varepsilon_r \sin\beta - \sqrt{\varepsilon_r + \cos^2\beta}} \tag{4}$$

2.3 Polarization adaptation

The main idea of adaptive polarization is to have primary (dominating) and secondary polarization in each cell. Primary polarization is valid for the whole service area of the cell whereas secondary polarization is only used in close proximity to the antenna, as presented in Fig. 2. Dominating polarization is planned in such a way that neighbor cells should use orthogonal polarization, as in Fig. 2. This adaptive polarization can be easily planned in small cells along highways. In traditional macro sites implemented on rooftops, it is challenging to plan the use of adaptive polarization, however, the reuse of orthogonal polarization can be planned for 6-sector site configuration, as presented in Fig. 3. As previously mentioned, multiple polarizations can only be used to achieve high data rates by using spatial multiplexing in close proximity of the antenna. The performance of polarization adaptation mostly depends on polarization change between dominating orthogonal polarizations in neighbor cells. This polarization change is measured in the following sections.

3 Measurement setup

For this research, outdoor measurements were conducted at Tampere University, Finland. During the measurements, the received signal strength was measured for different polarization configurations. In the first part, measurements were done with antennas having vertical and horizontal

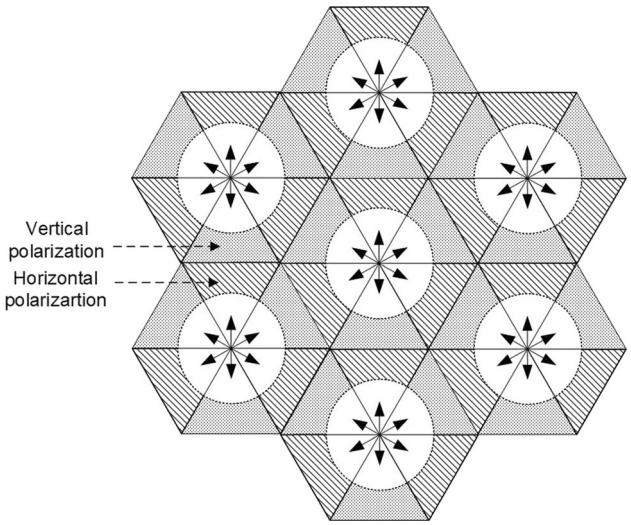

Fig. 3 Reuse of orthogonal polarizations in 6-sector macro sites

polarization, and four cases were considered: both TX and RX antenna with horizontal polarization (HH), the TX antenna with horizontal and RX antenna with vertical polarization (HV), both TX and RX antenna with vertical polarization (VV), and the TX antenna with vertical and RX antenna with horizontal polarization (VH). Similar wide beam antennas were used at TX and RX to capture the reflections from the building walls nearby, as shown in Fig. 4. The horn antenna had approximately 13 dBi antenna gain, and 40° of half power beamwidth (HPBW) in both vertical and horizontal planes. The horn antenna was able to transmit and receive with only a single polarization. Therefore, for transmitting and receiving with other polarizations, the antenna was physically turned by 90°. Both TX and RX antennas were placed two meters above the ground, as shown in Fig. 4(a).

Measurements were done for four different TX–RX separation distances: 7.5, 30, 45, and 60 m. Carrier measurements were performed at 1 GHz, 2 GHz and 3.4 GHz frequency bands. The three frequency bands targeted in this work were 970−1030 MHz, 2000−2030 MHz, and 3364−3400 MHz. At each frequency band, several measurement samples were collected over the frequency bandwidth to analyze the characteristics of fast fading in LOS propagation channels. Moreover, each measurement was repeated four times to average out any abnormal readings. The transmitting power was set to 15 dBm for all three frequency bands, and the receiver sensitivity (noise floor) was − 92 dBm. It was intended to keep the received signal level above the noise floor in all cases, and frequencies were selected to avoid external interference.

We have considered two different measurement environments in this paper. The first measurement scenario refers to a typical small cell environment in an urban street

(a)

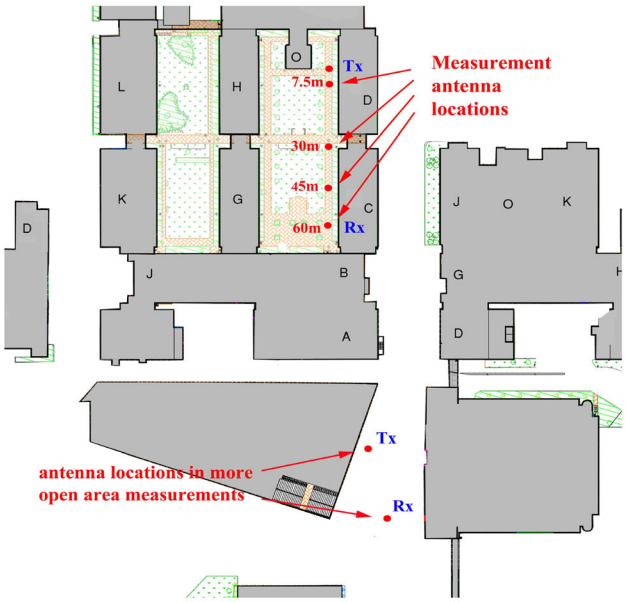

(b)

Fig. 4 Measurement setup in a street canyon environment, **a** Scenario, and **b** Layout

where building walls exist close to the transmitter and receiving antennas, as shown in Fig. 4(b). It also represents a practical pedestrian case or a lamp post small cell case. It should be noted that the building walls had rough surfaces. In the urban street environment considered, both TX and RX antennas were located nearly three meters away from the closest building wall. The second environment considered was categorized as an open area, as highlighted in Fig. 4(b). The same measurement setup was used for the open space as well. The RX antenna was located nearly 15 m away from the closest building wall, and hence strong nearby reflected paths were not present. The measurement environment was not changed so there is no impact of other moving objects. In the second part of the measurement campaign, urban street and open space environment measurements were repeated with a Kathrein K742222 antenna, which can support +/− 45° dual polarization. The target was to compare the performance of horizontal and vertical polarization with slanted +/− 45° polarization in terms of XPD. The Kathrein K742222 antenna does not support the 3.4 GHz band, therefore, measurements were only done for 1 and 2 GHz bands. A detailed data sheet of the Kathrein K742222 antenna is provided in reference [12].

4 Measurement results and discussion

The main goal of the measurements was to evaluate cross-polarization discrimination ratio in a small cell environment, which is mainly dominated by the LOS path. The quality of the measurement data was taken into account while post-processing the measurement data. Each measurement was repeated four times, and all measurement samples were considered during the analysis.

Initially, the impact of small frequency change is analyzed, and for this purpose, the measurement samples from the 970–1030 MHz frequency band with a TX-RX separation of 30 m was considered. Figure 5 shows the received power levels of different horizontal/vertical polarization configurations at TX and RX for the 970–1030 MHz frequency band, with a TX–RX separation of 30 m in the urban street and open area environments. It can be seen in Fig. 5(a, b) that the received signal strength is fairly stable for HH and VV polarization configurations. It was found that the standard deviations (STDs) of the received power levels of HH and VV configurations in the urban street environment were 0.77 dB and 0.84 dB, respectively, whereas in the open area environment, the STDs for HH and VV configurations were even lower at 0.42 dB and 0.44 dB, respectively. It can be seen in Fig. 5(a, b) that the received power levels of HV and VH configurations in both urban street and open area environments are much lower compared with HH and VV polarization configurations, and they fluctuate more. The STDs of the received power level of HV and VH configurations in the urban street environment are 3.59 dB and 2.1 dB, respectively, whereas in the open area environment, the STDs of HV and VH configurations are 6.41 dB and 3.38 dB, respectively. These results presented include the impact of fast fading along with the impact of

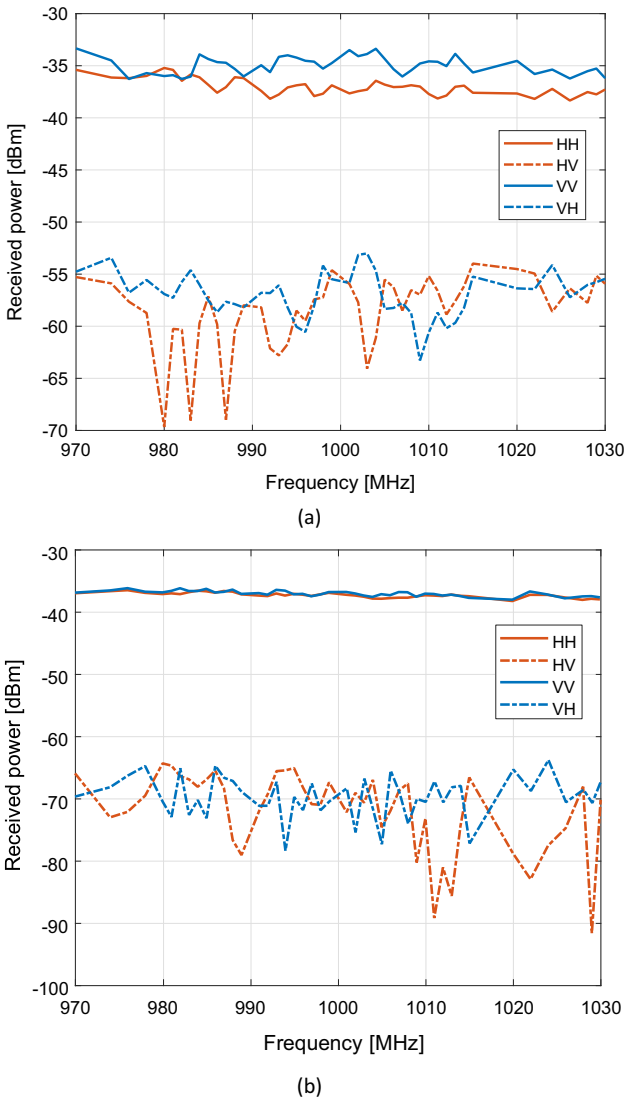

Fig. 5 Measurement samples at 970−1030 MHz in cases of HH, HV, VV, and VH at a 30 m distance in **a** Street canyon and **b** Open area environments

polarization turning due to the environment. As expected, it was found that the received power levels with HV and VH polarization configurations are significantly lower than HH and VV configurations.

The mean values of the received signal strength of HH, HV, VV, and VH polarization configurations, and XPD ratio at 970–1030 MHz with 30-m TX-RX separation are given in Table 1. Interestingly, it was found that the XPD ratio for both HH–HV and VV–VH configurations is around 22 dB in the street canyon environment but there is a higher XPD ratio of around 32.6–34.7 dB in an open area environment. It should be noted that there were no nearby walls at RX in the open area environment, and thus there was less change in polarization in the open area environment compared with the urban street environment, which results in increased XPD ratio. It can be seen from the results presented in Table 1 that the multipath-rich environment (urban street) offers lower XPD ratio compared with a less multipath-rich environment (open area).

As the main focus of this research work was to study XPD ratio, in the next phase, we investigated the change in XPD ratio from small changes in TX-RX separation and frequency. TX-RX separation distances of 27, 28, 29, and 30 m were measured in the urban street and open area environments to check local variations in XPD ratio. Figure 6 shows the XPD ratio of different polarization configurations at three frequencies, 1, 2, and 3.4 GHz. As previously discussed, it can be seen from Fig. 6(a, b) that the mean value of XPD is higher in an open area environment than the urban street environment at all considered distances, due to less availability of strong reflected paths from the nearby walls. Moreover, the STDs of XPD ratio in each frequency band is between 0.3−7.5 dB and 0.4−4.5 dB for urban street and open area environments, respectively. These results indicate that XPD is unique at each location, and there is less variation in cases where reflections have less influence on the total received power.

Figure 7 shows the mean values of XPD ratio at different distances in the urban street environment for 1, 2, and 3.4 GHz operation frequencies. The results presented in Fig. 7 show that the mean value of XPD ratio may remarkably change with the change in distance as well as with the change in frequency. For example, at 3.4 GHz frequency, the XPD ratio of the HH–HV configuration is around 42 dB, 14 dB, 26 dB and 22 dB at distances of 7.5, 30, 45 and 60 m, respectively. From Figs. 6 and 7, it can also be noted that XPDs in both cases of HH–HV and VV–VH are also changed with the change in frequency. Furthermore, XPD ratio is not linearly dependent on frequency and distance, rather it depends upon the intensity of the reflected paths available. Considering all measured XPD ratio results from horizontal/vertical polarization at 1, 2, and 3.4 GHz frequencies, the mean values of XPD ratio were around 24.7 dB and 31.7 dB in the urban street and open area environments, respectively.

In the second part of this research work, measurements were done with +/− 45° slanted antennas. Figure 8 shows the received power level of different TX–RX configurations utilizing an antenna with +/− 45° slanted polarization at the 970–1030 MHz frequency band with a TX–RX separation of 30 m in the urban street and open area environments. Before discussing the results presented in Fig. 8, it is important to highlight here that the receiving antenna was facing towards the TX antenna. Therefore, the notations used for +/− 45° slanted polarizations are reversed at the RX end, unlike horizontal/vertical polarization. For example, in Fig. 8, the notation OV represents the case of TX and RX antenna with + 45° and OO

Table 1 Mean RX level and XPD ratio at 970−1030 MHZ with 30 m TX-RX separation and horizontal/vertical polarization

	Mean RX level (dBm)				XPD ratio (dB)	
	HH	HV	VV	VH	HH–HV	VV–VH
Street canyon	− 37.0	− 58.6	− 35.0	− 57.0	21.6	22.0
Open area	− 37.3	− 70.4	− 37.2	− 69.5	34.7	32.6

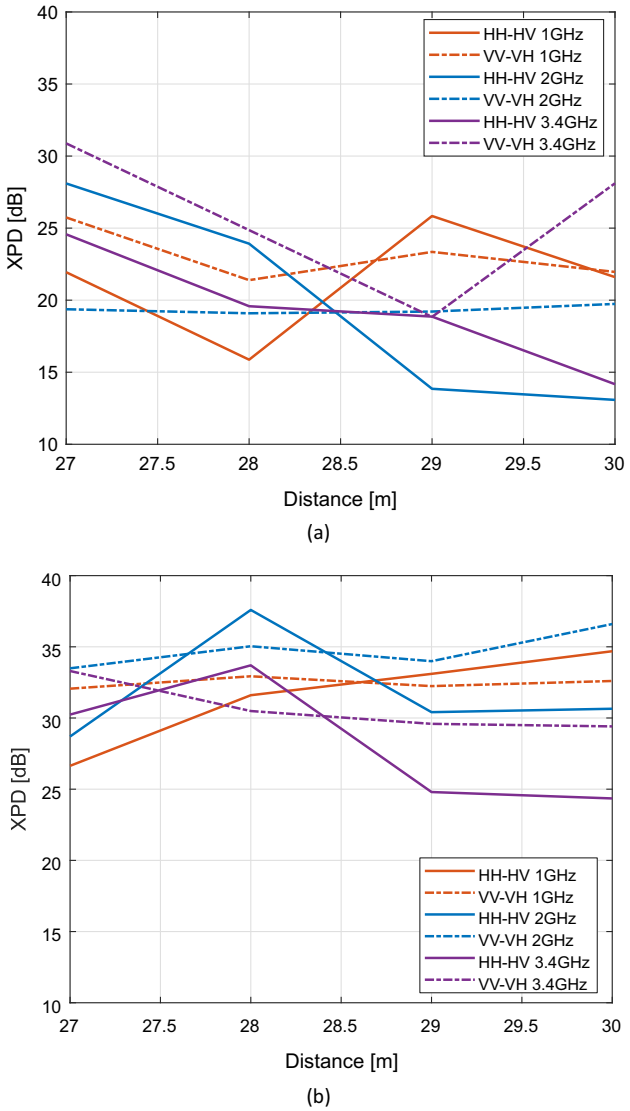

Fig. 6 Local variation of XPD for antenna with horizontal/vertical polarization at a distance of 27−30 m in **a** Street canyon and **b** Open area environments

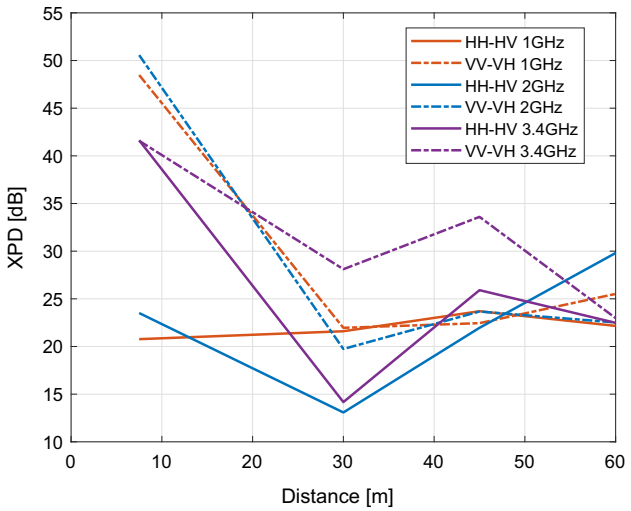

Fig. 7 Average XPD isolation with horizontal/vertical polarization at different distances and frequencies in an urban street environment

represents the case of TX and RX antenna with + 45° and − 45°, respectively. The notation VO represents the case of both TX and RX with − 45°, and VV represents the case of TX and RX with − 45° and + 45°, respectively. It was found that the STDs of the received power levels of OV and VO configurations in the urban street environment are 0.9 dB and 0.76 dB, respectively. In an open area environment, the STDs of the received power levels of OV and VO configurations are almost the same as in the urban street, and the reported values are 1.04 dB and 0.92 dB, respectively. Furthermore, the STDs of the received power levels of OO and VV configurations in the urban street environment are 2.3 dB and 1.8 dB, respectively. Surprisingly, the received power level fluctuates more for OO and VV configuration in an open environment, as can be seen in Fig. 8(b), and the STDs of the received signal power in an open area for OO and VV configurations were around 5.8 dB and 5.4 dB, respectively.

The mean values of the received signal strengths and XPD ratios for different configurations with +/− 45° slanted polarization antennas at 970–1030 MHz and 30-m TX–RX separation are given in Table 2. The XPD ratio was similar in open and street environments and was in the range of 8.6–11.2 dB. However, the results presented in Table 1 showed more XPD ratio in an open area environment compared with a street environment in the case of horizontal/vertical polarization.

Figure 9 shows the mean values of XPD ratio at different distances in the urban street environment for 1 and 2 GHz frequencies. A similar random response of XPD ratio was observed with slanted polarization as received with horizontal/vertical polarization. The XPD ratio of OO–OV and VV–VO configuration changed considerably with changes in distance and frequency. Considering all

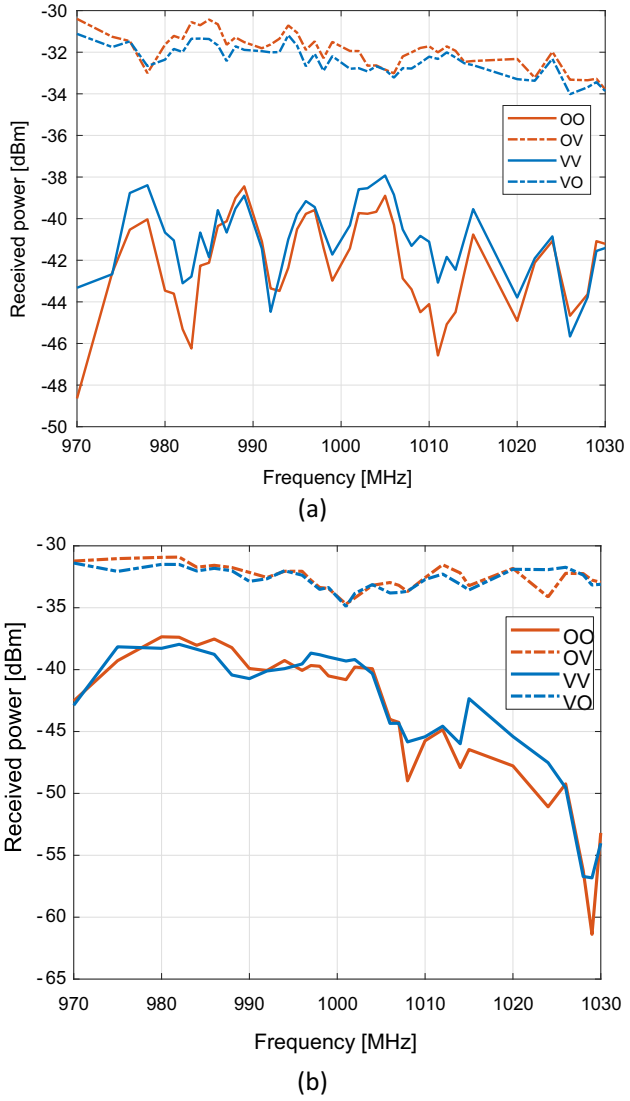

Fig. 8 Measurement samples at 970−1030 MHz in cases of OO, OV, VV, and VO at a 30 m distance in **a** Street canyon and **b** Open area environments

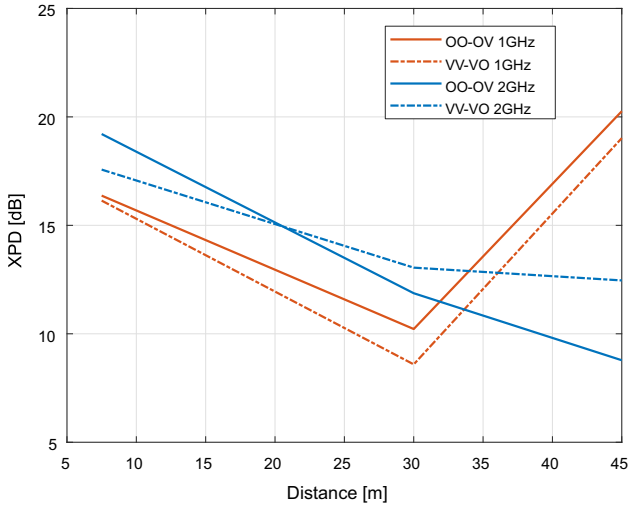

Fig. 9 Average XPD isolation with +/−45 slanted polarization at different distances and frequencies in an urban street environment

measured XPD results from +/− 45° slanted polarization at frequencies of 1 and 2 GHz, mean values of XPD ratio were found to be around 11.5 dB and 12.1 dB in the urban street and open area environments, respectively. It is evident by comparing the results presented in Figs. 7 and 9 that the horizontal/vertical polarization yields greater XPD ratio, i.e., more isolation, compared with the +/− 45° slanted polarization.

The results provided the expected range of XPD ratio in a small cell urban street environment and open areas with horizontal/vertical, and +/− 45° slanted polarization. In streets, the immediate neighbor cell is the major contributor to the interference at the cell edge. Therefore, at the cell border area, the XPD ratio may represent the signal-to-interference ratio. In this way, XPD ratio can be used to estimate the maximum supported bitrate at the cell border area. The maximum supported data rate T can be estimated by using Shannon's capacity formula given in Eq. 5, where N_B is the number of parallel bit streams, B is the system bandwidth in Hertz, SIR is the signal to interference ratio in a linear scale.

$$T = N_B B Log_2(1 + SIR) \tag{5}$$

Assuming the received signal strength is clearly above the noise floor level, and considering 1 Hz of bandwidth, and 25 dB of SIR (referring to the average XPD of 24.7 dB with horizontal/vertical polarization in an urban street), the Shannon equation yields a data rate of 8.3 bps. Whereas for an SIR of 0 dB, i.e., the cell border area considering the utilization of the same polarization in the neighbor cell, the Shannon equation gives a spectral efficiency (SE) of 1bps. Thus, the 25 dB of improvement in SIR achieved by utilizing orthogonal polarization at the neighbor cell offers more than an 800% improvement in throughput at the cell border area compared with a cell utilizing the same polarization in the neighbor cell with a single bit stream. It should be noted that the SIR distribution heavily depends on the base station antenna configurations and antenna radiation patterns.

For ease of understanding, the performance gain of polarization adaptation is compared with a traditional case in an example calculation where the same polarization is used in the neighbor cell and with a widely used MIMO 2 × 2 configuration utilizing two orthogonal polarizations, e.g., horizontal and vertical, in the same cell. We consider a simple system of two cells with omnidirectional antennas, and the worst-case scenario is considered such that there exists an LOS connection between the UE and the serving base and the interfering base station, whereas the impact of

Table 2 Mean RX level and XPD ratio at 970−1030 MHZ with 30 m TX–RX separation and + /− 45 ° slanted polarization

	Mean RX level (dBm)				XPD ratio (dB)	
	OO	OV	VV	VO	OO–OV	VV–VO
Street canyon	− 42.2	− 32.0	− 41.1	− 32.5	10.2	8.6
Open area	− 43.8	− 32.6	− 43.5	− 32.8	11.2	10.7

Table 3 Spectral efficiency of different configurations in two cell scenario in LOS channel

Distance [m]	SIR normal [dB]	SISO SE [bps]	MIMO 2 × 2 SE [bps]	SIR orth pol [dB]	Orth pol SE [bps]	Orth + MIMO 2 × 2 SE [bps]
10	25.57	8.50	17	25	8.3	17
20	19.08	6.35	12.7	25	8.3	12.7
30	15.06	5.05	10.1	25	8.3	10.1
40	12.04	4.09	8.18	25	8.3	8.3
50	9.54	3.32	6.64	25	8.3	8.3
60	7.35	2.69	5.37	25	8.3	8.3
70	5.37	2.15	4.3	25	8.3	8.3
80	3.52	1.70	3.4	25	8.3	8.3
90	1.74	1.32	2.64	25	8.3	8.3
100	0	1.00	2	25	8.3	8.3

the antenna radiation pattern is ignored. It is assumed that the inter-cell distance is 200 m, and an FSPL model given in Eq. 1 is used to compute path loss at any given point.

Table 3 provides the SIR and expected SE at a given distance from the serving BS for three cases, traditional SISO, MIMO 2 × 2, and the polarization adaptation approach. In Table 3, it should be noted that the SIR for the case of utilizing orthogonal polarization in neighbor cells is fixed at 25 dB, which corresponds to the fixed SE of 8.3bps. In Table 3, at a distance of 10 m from the BS, the reported SIR value for traditional SISO and MIMO 2 × 2 systems utilizing the same polarization in neighbor cells is 25.57 dB, which has a SE of 8.5bps and 17bps for SISO and MIMO 2 × 2, respectively. It can be seen in Table 3 that the SIR in the normal case degrades with the increase in distance, and at the cell border area (assuming 200 m inter-cell distance) the $SIR = 0$ dB, and that yields a SE of only 1bps and 2bps for SISO and MIMO 2 × 2, respectively. It should be noted that MIMO 2 × 2 is able to provide better SE compared with polarization adaptation for distances up to 30 m, which is only 30% of the cell area in our sample calculation. Polarization adaptation provides better SE for the rest of the cell coverage area, which is 70% of the cell area. Therefore, an adaptation between MIMO 2 × 2 utilization and single orthogonal polarization could enhance the overall spectral efficiency of the cell, where 70% of the cell area is covered with single orthogonal polarization, and MIMO 2 × 2 is used in the remaining 30% of the cell area. Finally, the average SE of a cell is 7.23 bps and 9.79 bps for traditional MIMO 2 × 2 and polarization adaptation, respectively. This means that the overall cell capacity can be increased by almost 35% by utilizing polarization adaptation compared with MIMO 2 × 2.

5 Conclusions

The main goal of this research work was to highlight the impact of polarization adaptation on bitrates and system capacity in an outdoor small cell scenario in mobile networks. Through a series of measurements, a cross polarization discrimination (XPD) ratio was measured for different configurations of polarizations at the transmitter and receiver. We have considered horizontal, vertical, +/− 45° slanted polarization to investigate the differences. A two-cell model was the main focus of the measurements and therefore, other cell interference was excluded. Measurement results revealed that the mean value of XPD ratio may change significantly with the change in distance as well as with the change in frequency of operation and is not a linear function of them. It was found that there is greater XPD ratio in an open environment than in close proximity of walls. Considering all measured XPD ratio results for horizontal/vertical polarization at 1, 2, and 3.4 GHz frequencies, the mean values

of XPD ratios were around 24.7 dB and 31.7 dB in the urban street and open area environments, respectively. For +/− 45° slanted polarization at 1 and 2 GHz frequencies, the mean values of XPD ratios were around 11.5 dB and 12.1 dB in the urban street and open area environments, respectively.

Later, considering a simple two-cell model, the performance gain of polarization adaptation was compared with a traditional case where the same polarization is used in the neighbor cell and with a widely used MIMO 2 × 2 configuration utilizing two orthogonal polarizations, horizontal and vertical, in the same cell. It was found that MIMO 2 × 2 is able to provide better spectral efficiency (SE) compared with polarization adaptation for 30% of the cell area whereas polarization adaptation provides better SE for the rest of the cell coverage area, which is 70% of the cell area. Therefore, an adaptation between MIMO 2 × 2 utilization and single orthogonal polarization could enhance the overall spectral efficiency of the cell. Finally, the average SEs of a cell were 7.23 bps and 9.79 bps for traditional MIMO 2 × 2 and polarization adaptation, respectively. This means that the overall cell capacity can be increased by almost 35% by utilizing polarization adaptation compared with just MIMO 2 × 2.

The optimal implementation of polarization adaptation should be studied in future research. These optimal implementation scenarios include both fixed beam and beam steering cases. The impact of antenna configurations, such as radiation pattern, the direction of the antenna in the azimuth plane, and down tilting, need to be studied. In future studies, work can also be extended to the orbital angular momentum technique which is one method offering new orthogonal channels in 6G mobile networks. Future studies can also be extended to highways where wide low SIR areas happen between sites, and where polarization turning/change is minimal due to a lack of scattering cross-sections. Finally, typical non-LOS (NLOS) areas from macro base stations need to be studied as this paper was mainly focusing on LOS scenarios.

Acknowledgements This work was supported in part by Aalto University and Tampere University. Measurements were supported by mobile operator DNA (Telenor Group).

Funding Open access funding provided by Tampere University (including Tampere University Hospital).

References

1. Saleh, A. M., Le, N. T., & Sesay, A. B. (2018) Inter-cell interference coordination using fractional frequency reuse scheme in multi-relay multi-cell ofdma systems. In *2018 IEEE Canadian conference on electrical and computer engineering (CCECE)* (pp. 1–5).
2. Assaad, M. (2008). Optimal fractional frequency reuse (ffr) in multicellular ofdma system. In *2008 IEEE 68th vehicular technology conference* (pp. 1–5).
3. Sheikh, M. U., Lempiäinen, J., & Jäntti, R. (2022). Capacity limitation of small cell densification. In *2022 International conference on information networking (ICOIN)* (pp. 210–214).
4. Yamada, S., Choudhury, D., Thakkar, C., Chakrabarti, A., Dasgupta, K., Daneshgar, S., & Horine, B. D. (2019). Cross-polarization discrimination and port-to-port isolation enhancement of dual-polarized antenna structures enabling polarization mimo. *IEEE Antennas and Wireless Propagation Letters, 18*(11), 2409–2413.
5. Sheikh, M. U., Jagusz, R., & Lempiäinen, J. (2011). Performance evaluation of adaptive mimo switching in long term evolution. In *2011 7th International wireless communications and mobile computing conference* (pp. 866–870).
6. Sarris, I., & Nix, A. R. (2007). Design and performance assessment of high-capacity mimo architectures in the presence of a line-of-sight component. *IEEE Transactions on Vehicular Technology, 56*(4), 2194–2202.
7. Hofmann, C. A., Ogermann, D., & Lankl, B. (2013). Measurement results for the comparison of multiple and single polarized mimo channels in los, nlos, indoor and outdoor scenarios. In *WSA 2013; 17th international ITG workshop on smart antennas* (pp. 1–8).
8. Castañeda Garcia, M. H., Iwanow, M., & Stirling-Gallacher, R. A. (2018). Los mimo design based on multiple optimum antenna separations. In *2018 IEEE 88th vehicular technology conference (VTC-Fall)* (pp. 1–5).
9. Padgett, M. J. (2017). Orbital angular momentum 25 years on. *Optics Express, 25*(10), 11265–11274.
10. Saunders, S. R., & Simon, S. R. (1999). *Antennas and propagation for wireless communication systems* (1st ed.). Wiley.
11. Höijer, M. (2013). Polarization of the electromagnetic field radiated from a random emitter and its coupling to a general antenna. *IEEE Transactions on Electromagnetic Compatibility, 55*(6), 1335–1337.
12. "Kathrein | 742222V01—Datasheet PDF Tech Specs.https://www.datasheets.com/en/part-details/742222v01-kathrein-51601935

Jukka Lempiäinen was born in Helsinki, Finland, in 1968. He received his M.Sc., Lic. Tech. and Dr. Tech. degrees, all in electrical engineering, from Helsinki University of Technology (today Aalto University), Espoo, Finland, in 1993, 1998, and 1999, respectively. He has served in Tampere University (Finland) as a Professor since 2001. For his entire career, he has concentrated to improve the principles of radio planning in cellular networks. Lempiäinen has especially focused on an optimal definition of Radio Access Network (RAN) infrastructure including critical communication. Recently, Lempiäinen has actively studied the techno-economical balance of different radio systems as terrestrial networks (Mobile), local area networks (WiFi) and satellite networks. Lempiäinen is URSI national board national board member, Finland.

Muhammad Usman Sheikh was born in Rawalpindi, Pakistan, in 1983. He received his B.Sc. degree in Electrical Engineering from CIIT Islamabad, Pakistan in 2006. He received his M.Sc., and D.Sc. (Tech) degrees from Tampere University of Technology (TUT), Finland in 2009 and 2014, respectively. Currently, he is working as a part-time post-doctoral researcher at Aalto University, Finland. He has more than 10 years of experience from different radio network planning and optimization projects. His general interests include network planning and optimization, future mobile technologies, radio propagations, channel modeling, 3D ray tracing, advanced antennas and novel and innovative cellular concepts. He is the author of several international journal articles, conference papers, and book chapters and he is a senior IEEE member.

Ari Asp has received his M.Sc. degrees from the Tampere University of Technology in 2002. Now he has written his dissertations on the topic of signal attenuation by concrete element walls of apartment buildings. Since 2003, he has worked mainly in teaching positions in the area of wireless communication technology, but at the same time his research focuses on modelling wireless measurement systems as well as studying radio wave propagation. He has extensive experience performing channel measurements at a variety of frequency bands between 800 MHz and 30 GHz and study electrical parameters to building construction materials. During his dissertation work, he has participated extensively in the social debate about the problems caused by the weak signal level of residential buildings.

Riku Jäntti is a Full Professor in Communications Engineering at the Department of Information and Communications Engineering, Aalto University School of Electrical Engineering, Finland. He received his M.Sc. (with distinction) in Electrical Engineering in 1997 and D.Sc (with distinction) in Automation and Systems Technology in 2001, both from Helsinki University of Technology (TKK). Prior to joining Aalto (formerly known as TKK) in August 2006, he was professor pro tem at the Department of Computer Science, University of Vaasa. Prof. Jäntti is a senior member of IEEE and associate editor of IEEE Transactions on Vehicular Technology. The research interests of Prof. Jäntti include machine type communications, low-power wireless systems, cloud based radio access networks, and quantum communications.